Investigation of the first and second dehydroxylation of kaolinite

Petra Zemenová · Alexandra Kloužková ·
Martina Kohoutková · Robert Král

Abstract Raw material kaolin Sedlec Imperial and four
types of rehydroxylated samples were used to study the
processes of the first and second dehydroxylation of kao-
linite by thermal analysis and IR spectroscopy. Activation
energy (E_a) of these processes was calculated from DSC
curves using five isoconversional methods. IR spectroscopy
was used to compare structures of the original and rehy-
droxylated samples. It was proven that the structure of
rehydroxylated metakaolinite can closely resemble that of
the raw kaolinite under intensive hydrothermal treatment
but does not reach the original structure. The E_a values of
the second dehydroxylation reach 87–92 % of E_a values of
the first dehydroxylation.

Keywords Kaolinite · Dehydroxylation ·
Rehydroxylation · Thermal analysis · Kinetics

P. Zemenová (✉) · A. Kloužková
Department of Glass and Ceramics, ICT Prague, Technická 5,
166 28 Prague, Czech Republic
e-mail: petra.zemenova@vscht.cz

A. Kloužková
e-mail: alexandra.klouzkova@vscht.cz

M. Kohoutková
Central Laboratories, ICT Prague, Technická 5, 166 28 Prague,
Czech Republic
e-mail: martina.kohoutkova@vscht.cz

R. Král
Institute of Physics of the Academy of Sciences of the Czech
Republic, Cukrovarnická 10, 162 00 Prague, Czech Republic
e-mail: kralr@fzu.cz

Introduction

Kaolinite ($Al_2O_3 \cdot 2SiO_2 \cdot 2H_2O$) is a two-layer clay mineral
lying between dioctahedral 1:1 phyllosilicate. Crystals of
kaolinite are hexagonal in shape and are formed by layers
of the tetrahedral $[SiO_4]^{4-}$ and layers of the octahedral
$[Al(OH)_6]^{9-}$ which alternate periodically [1]. Water is
bound in the form of four hydroxyl groups in each unit cell.
The inner hydroxyl group lies between tetrahedral and
octahedral sheet, while three inner-surface hydroxyl groups
lie between adjacent kaolinite layers [2]. Characteristic
positions of kaolinite peaks in the infrared spectrum (ATR-
ZnSe crystal) are found at 3620 cm^{-1} for inner hydroxyl
group and at 3650, 3671 and 3695 cm^{-1} for inner-surface
hydroxyl groups. In case of the kaolinite structure with
lower degree of ordering, peaks at 3650 and 3671 are
replaced by one peak at the position of 3651 cm^{-1} [2, 3].

When kaolinite is heated, it loses any physically
absorbed water between 100 and 200 °C, i.e. dehydration
occurs. Kaolinite transforms to an unstable non-crystalline
product, metakaolinite ($Al_2Si_2O_7$), after calcination at 450–
600 °C, by losing the chemically bound water molecules
[4, 5]:

$$Al_2O_3 \cdot 2SiO_2 \cdot 2H_2O \rightarrow Al_2O_3 \cdot 2SiO_2 + 2H_2O.$$
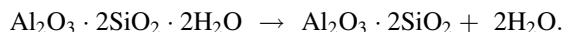
Hydroxyl groups in kaolinite structure are released in
two steps. At first, the hydroxyl groups from the surface
layer are released, and subsequently the release of inner
hydroxyl groups occurs [6]. This process is called dehy-
droxylation and is accompanied by a mass loss of
approximately 14 mass % as estimated from the theoretical
composition (46.54 mass % SiO_2, 39.5 mass % Al_2O_3 and
13.96 mass % H_2O) [1]. The process of dehydroxylation is
characterised by endothermic effect at curves measured by
thermal analysis (DTA or DSC). Exact positions of this

Table 1 Equations for the calculation of activation energy

Kissinger method	[17, 21]

$$\ln \frac{\beta}{T_{\mathrm{m}}^2} = C - \frac{E_{\mathrm{a}}}{R T_{\mathrm{m}}}$$

Kissinger–Akahira–Sunose method	[18]

$$\ln \frac{\beta}{T_{\alpha}^2} = C - \frac{E_{\mathrm{a},\alpha}}{R T_{\alpha}}$$

Flynn–Wall–Ozawa method	[18, 22]

$$\ln \beta = C - \frac{1.0518\, E_{\mathrm{a},\alpha}}{R T_{\alpha}}$$

Starink method	[18]

$$\ln \frac{\beta}{T_{\alpha}^{1.92}} = C - \frac{1.0008\, E_{\mathrm{a},\alpha}}{R T_{\alpha}}$$

Tang method	[19]

$$\ln \frac{\beta}{T_{\alpha}^{1.894661}} = C - \frac{1.00145033\, E_{\mathrm{a},\alpha}}{R T_{\alpha}}$$

T_{m} Temperature of peak (K), T_{α} Temperature of the degree of conversion α (K), β Heating rate (K min^{-1}), R Gas constant (8.314 J K^{-1} mol^{-1}), E_{a} Activation energy (kJ mol^{-1}), C Constants

effect are influenced by particle size, structure ordering of kaolinite and also by heating rate [7, 8]. Partial dehydroxylation can occur already during the processing of raw materials containing kaolinite, e.g. dry grinding [9, 10].

Processes of rehydration and rehydroxylation are reverse to dehydration and dehydroxylation processes of kaolinite. They occur immediately after low-temperature calcination (below ca. 1,000 °C) of ceramics prepared from clay raw materials by the influence of moisture. At first, physically absorbed water,

which was lost during heating at 100–200 °C, is regained, i.e. rehydration occurs. It is followed by rehydroxylation—recovering of structural hydroxyl groups, during long-time influence of moisture [11–15]. The first reaction of atmospheric moisture with the fired clay is called first rehydroxylation. The second dehydroxylation and subsequent second rehydroxylation can occur when kaolinite is heated repeatedly and then exposed to atmospheric moisture.

The kinetics of dehydroxylation can be studied by several analytical methods (XRD, IR, TA). Thermal analysis can proceed under isothermal or non-isothermal conditions. Dehydroxylation of kaolinite is a reaction of A(s)→B(s) + C(g) type. Using thermal analysis for studying kinetic parameters, non-isothermal conditions are often applied. Kinetic parameters can be calculated by simple model-free and isoconversional methods or by more complicated methods based on the direct mechanism [16]. Kissinger method is a well-known model-free method (Table 1) [17]. Using isoconversional methods (e.g. Kissinger–Akahira–Sunose, Flynn–Wall–Ozawa, Starink, Tang (Table 1) [18–22]), activation energy is calculated via degree of conversion, which is constant with values from 0 to 1. The degree of conversion can be calculated from the mass difference at TG curve or by the integration of peak areas from DTA or DSC curves. Activation energy values of the kaolinite dehydroxylation usually range from 140 to 240 kJ mol^{-1} [6, 21–23].

Table 2 Chemical composition of the raw material [mass %]

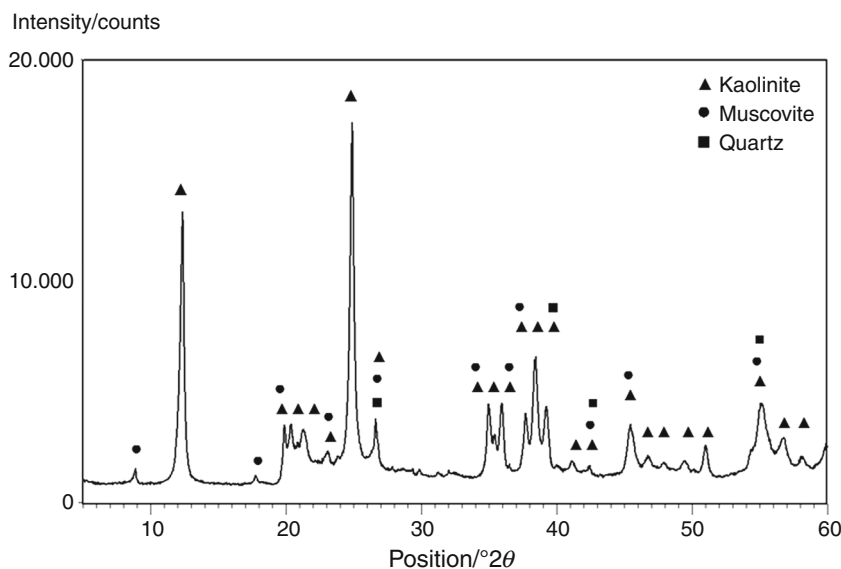| Composition	SiO$_2$	Al$_2$O$_3$	Fe$_2$O$_3$	TiO$_2$	CaO	MgO	K$_2$O	Na$_2$O
Content/mass %	49.89	46.89	1.10	0.30	0.40	0.30	1.10	0.03

Fig. 1 XRD pattern of raw material

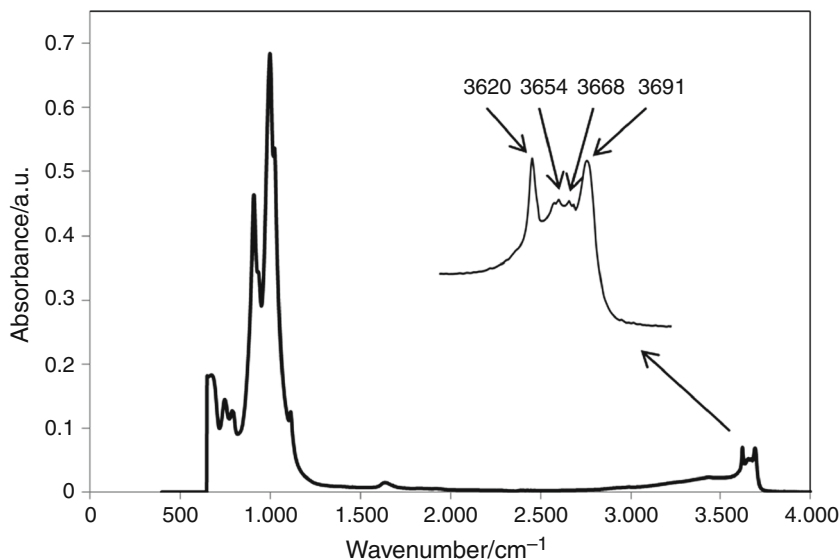**Fig. 2** Infrared spectra of the raw material

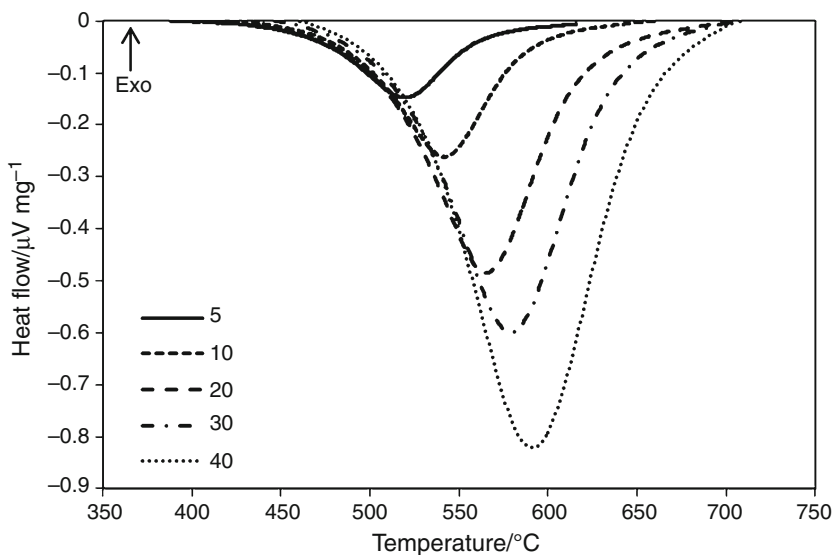**Fig. 3** DSC curves of the raw material at different heating rates

Table 3 Values of the temperature of peak extremum for the first dehydroxylation

Heating rate/K min^{-1}	5	10	20	30	40
Temperature of peak extremum/ °C	518	541	565	578	597
TG/mass %		12.08	12.10	12.09	12.09	12.10

The aim of this work was to study the process of kaolinite dehydroxylation using thermal analysis and to compare activation energies of the first and second dehydroxylation.

Experimental

Kaolin Sedlec Imperial (Czech Republic) in the form of well-dried gently ground powder was used as the raw material. It was heated in a Pt crucible in a laboratory furnace at the rate of 10 K min^{-1}. The choice of calcining conditions (C)—2 h at 600 °C and 96 h at 450 °C—was based on previous research [24]. Products of calcinations were subsequently hydrothermally treated (HA) in laboratory autoclaves at 230 °C (2.77 MPa) for 10 and 100 h. A solid/solution ratio of 1 g sample/20 mL water was used in the experiments. All samples were dried until a constant mass (2 h at 105 °C) was attained before IR and thermal analyses.

Fig. 4 DSC curves of the raw material and hydrothermally aged samples at the heating rate of 10 K min^{-1}
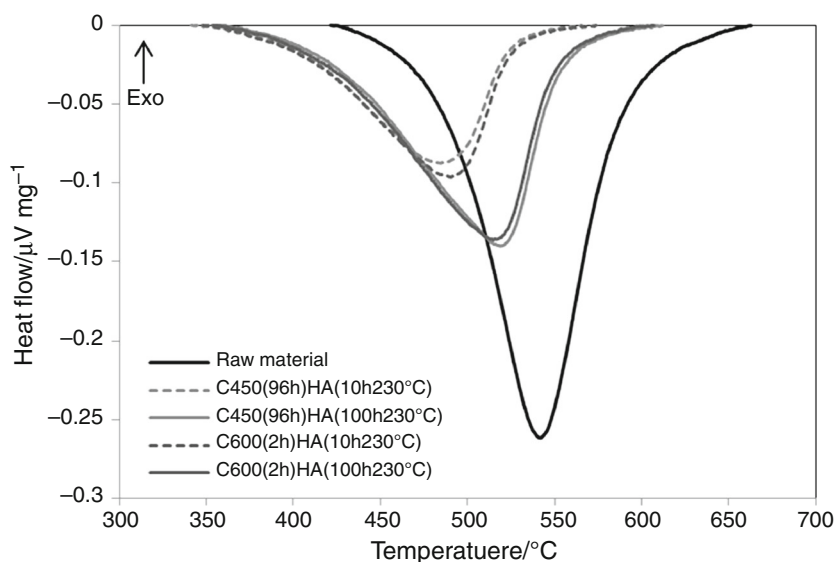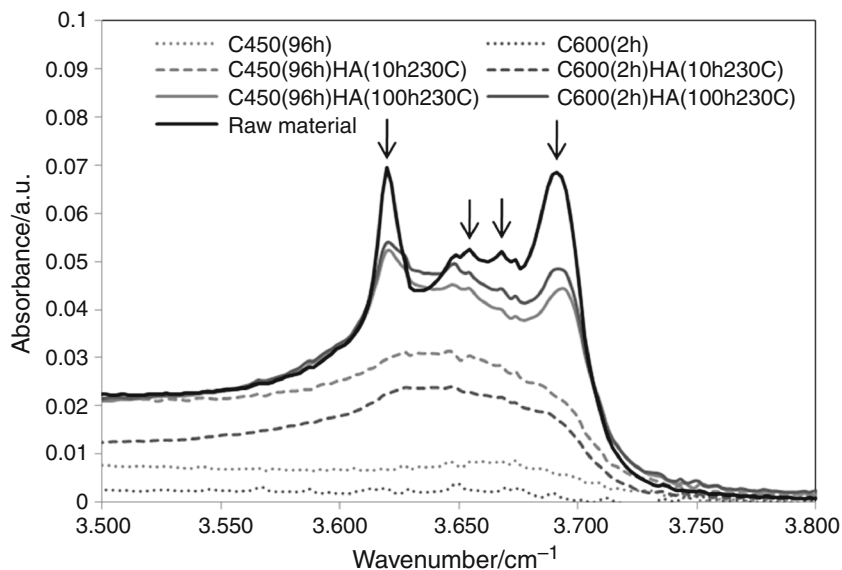

Fig. 5 Infrared spectra of the raw material and hydrothermally aged samples

The chemical composition of the raw material was determined by X-ray fluorescence analysis (Sequential WD-XRF spectrometer ARL 9400 XP$^+$). The particle size distribution was evaluated by laser diffraction (Fritsch Analysette 22 NanoTec). X-ray diffraction analysis (Diffractometer PANalytical X'pert Pro) was used to identify accessory minerals in the raw kaolin sample. The structural ordering of the raw material and treated samples was characterised by infrared spectroscopy (spectrometer Nicolet IS 10, Thermo Scientific). Measured data were evaluated using programs Omnic and Origin. Thermal analyses were performed with a Setaram Setsys Evolution 16 system (DSC-TG) using 25 ± 0.02 mg of sample at the heating rates of 5, 10, 20, 30 and 40 K min^{-1} in the temperature range of 20–1200 °C in argon flow at atmospheric pressure. DSC data were used to calculate the activation energy of the dehydroxylation process using five methods listed in Table 1. The degree of conversion was calculated by the integration of endothermic peak area from the DSC curve. The percentage of kaolinite in samples was calculated from TG curves and related to its theoretical composition [25].

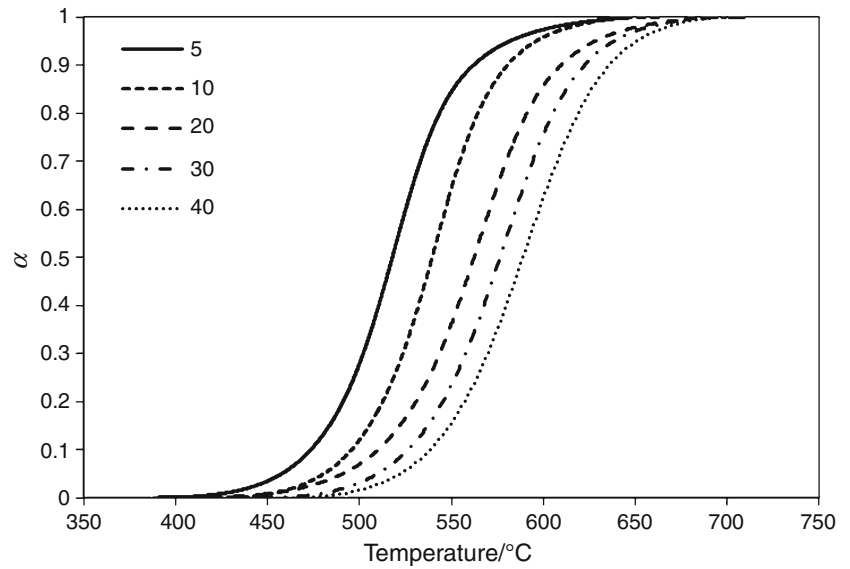**Fig. 6** Degree of conversion of the raw material at different heating rates

Fig. 7 Degree of conversion of the raw material (**1**) and hydrothermally aged samples (**2**) at the heating rate of 10 K min^{-1}
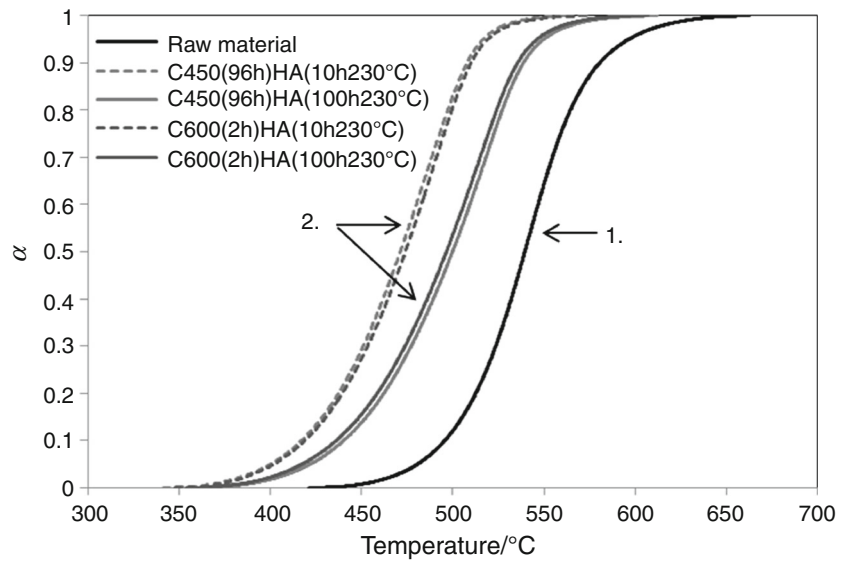

Table 4 Values of the activation energy for the first and second dehydroxylation

Method	1. Dehydroxylation activation energy/kJ mol^{-1}	2. Dehydroxylation activation energy/ % 600 °C (2 h)		2. Dehydroxylation activation energy/ % 450 °C (96 h)	
		10 h 230 °C	100 h 230 °C	10 h 230 °C	100 h 230 °C
Kissinger	149	94.0	105.4	92.5	98.9
Kissinger–Akahira–Sunose	157	87.9	92.1	87.4	89.6
Flynn–Wall–Ozawa	162	88.1	92.3	87.7	90.0
Starink	157	88.0	92.1	87.4	89.6
Tang	159	87.3	91.6	86.5	88.9

Results and discussion

The raw material (kaolin) is characterised by chemical composition of the main oxides recalculated to 100 mass % listed in Table 2 and particle mean value 3.2 μm. Raw material contains kaolinite as the main crystalline phase accompanied by small amount of quartz and mica (Fig. 1). The samples contained only quartz and mica after calcinations at 450 °C as well as at 600 °C. IR spectrum of kaolin with detailed positions of hydroxyl groups is shown in Fig. 2. The band at 3620 cm^{-1} belongs to inner hydroxyl group and bands at 3654, 3668 and 3691 cm^{-1} belong to inner-surface hydroxyl groups.

Figure 3 shows DSC curves of the first kaolinite dehydroxylation (raw material) measured at different heating rates. The extremum of peak shifts to higher temperatures, and the peak area increases with the increasing heating rate. All curves are symmetric, and the initial stage of the dehydroxylation process is very similar. The shape of the peak corresponds to the structure ordering and the value of the reaction order. The values of peak extremum for particular heating rates are listed in Table 3. The mass change measured at 10 K min^{-1} is 12.1 mass %, which corresponds to 86.9 % of kaolinite in the raw material.

Four types of rehydroxylated samples were used to study second dehydroxylation of kaolinite. The effect of calcination conditions and hydrothermal treatment on the structure and the amount of rehydroxylated kaolinite was monitored. Figure 4 shows dehydroxylation DSC curves of the raw material and the rehydroxylated samples at the heating rate of 10 K min^{-1}. The dehydroxylation of all rehydroxylated samples proceeded at lower temperatures compared to the raw material. The temperature of the extremum of peaks of the rehydroxylated samples shifts to lower temperature with the increasing disorder of the kaolinite structure. The curves of rehydroxylated samples are asymmetric, which are due to the decreasing structural order. The process of rehydroxylation of the studied samples is affected especially by the conditions of hydrothermal treatment, not by the conditions of calcination. The amount of kaolinite in hydrothermally treated samples was 50.7 % (C600 °C_HA10 h), 60.7 % (C600 °C_HA100 h), 51 % (C450 °C_HA10 h) and 57.9 % (C450 °C_HA100 h).

The structure of rehydroxylated samples was studied by IR spectroscopy (Fig. 5). It is obvious that the conditions of rehydroxylation have a strong effect on the degree of ordering of the kaolinite structure—i.e. on the existence and the distance of OH bonds. The IR spectra of the hydrothermally treated samples at 230 °C for 100 h very closely resemble that of the raw kaolinite, but do not reach the original structure. They show all four characteristic positions of hydroxyl groups, but do not reach the intensity of the raw material.

The kinetics of dehydroxylation was studied using five methods. Figure 6 shows degrees of conversion of the raw material at five different heating rates for the first dehydroxylation. Degrees of conversion for the first and second dehydroxylation at the heating rate of 10 K min^{-1} are compared in Fig. 7. Calculated values of the activation energies (E_a) of the first and second dehydroxylation are listed in Table 4. The E_a value of the first dehydroxylation calculated by Kissinger method was 149 kJ mol^{-1}. Using other four methods, the E_a value ranges from 157 to 162 kJ mol^{-1}, which is in good agreement with the literature data (176 kcal mol^{-1} [6], 195 kJ mol^{-1} [23] or 178 kJ mol^{-1} [26]). The activation energy was calculated also for four types of rehydroxylated samples. The E_a values of the second dehydroxylation are related to the corresponding E_a of the first dehydroxylation and presented in % in Table 4. Samples which were hydrothermally treated for 10 h at 230 °C reached approximately the same values of E_a. In the case of harsher conditions (100 h at 230 °C), the values of E_a were higher and closer to the E_a values of the raw kaolinite. With regard to the asymmetry of DSC curves for rehydroxylated samples, the Kissinger method was found unsuitable for comparing the first and second dehydroxylation.

Conclusions

It was proven that the process of dehydroxylation of rehydroxylated samples (second dehydroxylation) proceeds at lower temperatures compared to the dehydroxylation of the raw material (first dehydroxylation). The shift is influenced by the degree of ordering of the kaolinite structure. Using intensive hydrothermal treatment, the structure of the rehydroxylated metakaolinite resembles that of the kaolinite, but even after 100 h at 230 °C, it does not reach the original structure. The activation energy (E_a) value was calculated from DSC curves using five methods. The E_a values of the first dehydroxylation of kaolinite range from 149 to 162 kJ mol^{-1}. The E_a values of the second dehydroxylation reach 87–92 % of E_a values of the first dehydroxylation. Kissinger method was found unsuitable for describing dehydroxylation processes in kaolinite, while the other four methods provide comparable values.

References

1. Murray H. Applied Clay Mineralogy. Volume 2. Elsevier Science; 2007.
2. Madejová J. FTIR techniques in clay minerals studies. Vib Spectrosc. 2003;31:1–10.

3. Vaculíková L, Plevová E, Vallová S, Koutník I. Characterization and differentiation of kaolinites from selected Czech deposits using infrared spectroscopy and differential thermal analysis. Acta Geodyn Geomater. 2011;8(1):59–67.

4. Davies TW, Hooper RM. Structural changes in kaolinite caused by rapid dehydroxylation. J Mat Sci Lett. 1985;4(4):39–42.

5. Hanykýř V, Kutzendörfer J. Technologie Keramiky. Praha: Silikátový svaz; 2008.

6. Stoch L, Waclawska I. Dehydroxylation of kaolinite group minerals I. Kinetics of dehydroxylation of kaolinite and halloysite. J Therm Anal. 1981;20:291–304.

7. Castelein O, Soulestin B, Bonnet JP, Blanchart P. The influence of heating rate on the thermal behaviour and mullite formation from a kaolin raw material. Ceram Intern. 2001;27:517–22.

8. Kissinger HE. Variation of peak temperature with heating rate in differential thermal analysis. J Res Natl Bur Stand. 1956;57:217–21.

9. Redfern SAT. The kinetics of dehydroxylation of kaolinite. Clay Miner. 1987;22:447–56.

10. Kristóf J, Frost R, Kloprogge J, Horváth E, Makó É. Detection of four different oh-groups in ground kaolinite with controlled-rate thermal analysis. J Therm Anal Calorim. 2002;69:77–83.

11. Shoval S, Yadin E, Panczer G. Analysis of thermal phases in calcareous iron age pottery using FT-IR and Raman spectroscopy. J Therm Anal Calorim. 2011;104:515–25.

12. Wilson MA, Carter MA, Hall C, Hoff WD, Ince C, Savage SD, Mckay B, Betts IM. Dating fired-clay ceramics using long-term power law rehydroxylation kinetics. Proc R Soc A. 2009;465:2407–15.

13. Tosheva L, Mihailova B, Wilson MA, Carter MA. Gravimetric and spectroscopic studies of the chemical combination of moisture by as-fired and reheated terracotta. J Eur Ceram Soc. 2010;30:1867–72.

14. Bowen PK, Drelich J, Scarlett TJ. Modeling rehydration/rehydroxylation mass-gain curves from Davenport ceramics. J Am Ceram Soc. 2013;96(3):885–91.

15. Hall C, Hamilton A, Wilson MA. The influence of temperature o rehydroxylation [RHX] kinetics in archaeological pottery. J Archaeol Sci. 2013;40:305–12.

16. Saikia N, Sengupta P, Gogoi PK, Borthakur PC. Kinetics of dehydroxylation of kaolin in presence of oil field effluent treatment plant sludge. Appl Clay Sci. 2002;22:93–102.

17. Kissinger HE. Reaction kinetics in differential thermal analysis. Anal Chem. 1957;29:1702–6.

18. Starink MJ. The determination of activation energy from linear heating rate experiments: a comparison of the accuracy of isoconversion methods. Thermochim Acta. 2003;404(1):163–76.

19. Tang W, Liu Y, Zhang H, Wang C. New approximate formula for Arrhenius temperature integral. Thermochim Acta. 2003;408:39–43.

20. Dion P, Alcover JF, Bergaya F, Ortega A, Llewellyn PL, Rouquerol F. Kinetic study by controlled-transformation rate thermal analysis of the dehydroxylation of kaolinite. Clay Miner. 1998;33:269–76.

21. Sahnoune F, Saheb N, Khamel B, Takkouk Z. Thermal analysis of dehydroxylation of Algerian kaolinite. J Therm Anal Calorim. 2012;107(3):1067–72.

22. Mamleev V, Bourbigot S, Le Bras M, Lefebvre J. Three model-free methods for calculation of activation energy in TG. J Therm Anal Calorim. 2004;78:1009–27.

23. Ptáček P, Šoukal F, Opravil T, Havlica J, Brandštetr J. The kinetics analysis of the thermal decomposition of kaolinite by DTG technique. Powder Technol. 2011;208:20–5.

24. Zemenová P, Kloužková A, Kohoutková M. Ageing of low-firing prehistoric ceramics in hydrothermal conditions. J Process Appl Ceram. 2012;6(1):59–64.

25. Haq A, Iqbal Y, Khan MR. Phase and microstructural characterization of kaolin clays from north western Pakistan. J Park Mater Soc. 2009;3(2):77–90.

26. Prodanović D, Živković ŽD, Dumić M. The kinetics of dehydroxylation and mullitization of Zettlitz kaolin in the presence of Calcium(II) as an ingredient. Thermochim Acta. 1989;156:61–7.